



# Isolation and characterization of dental follicle–derived Hertwig’s epithelial root sheath cells

Ju Eun Oh<sup>1</sup> · Jin-Kyu Yi<sup>2,3</sup>

Received: 3 April 2020 / Accepted: 29 July 2020 / Published online: 4 August 2020  
© Springer-Verlag GmbH Germany, part of Springer Nature 2020

## Abstract

**Objectives** The aim of this study was the isolation and characterization of dental follicle–derived Hertwig’s epithelial root sheath cells (DF-HERSCs).

**Materials and methods** DF-HERSCs were isolated from dental follicle (DF)–derived single-cell suspensions. Their epithelial phenotypes were analyzed by Western blotting, polymerase chain reaction (PCR), and quantitative polymerase chain reaction (qPCR). Epithelial-mesenchymal transition (EMT) was induced in DF-HERSCs by treatment with transforming growth factor- $\beta$  (TGF- $\beta$ ) or fetal bovine serum (FBS)–added medium. Characteristics of DF-HERSCs were compared with normal human oral keratinocytes (NHOKs) and normal human epidermal keratinocytes (NHEKs). Osteogenic differentiation and mineralization of DF-HERSCs were analyzed by alkaline phosphatase (ALP) and Alizarin red staining. All experiments were conducted in triplicate.

**Results** Primary DF-HERSCs were isolated from DF. Epithelial phenotypes of DF-HERSCs were confirmed by morphological and Western blot analysis. PCR results demonstrated that the origin of DF-HERSCs was neither endothelial nor hematopoietic. Enamel matrix derivative (EMD)–associated genes were not expressed in DF-HERSCs. Treatment with TGF- $\beta$  and FBS-added medium triggered the progression of EMT in DF-HERSCs. The acquired potency of differentiation and mineralization was shown in EMT-progressed DF-HERSCs.

**Conclusions** DF contains putative populations of HERSC, named DF-HERSC. DF-HERSCs shared common characteristics with NHOKs and NHEKs.

**Keywords** Dental follicle–derived HERS cells · Cementogenesis · Regenerative endodontic procedures · HERSC-dMSC interactions

---

**Clinical relevance** Scientific evidence of the roles of DF-HERSCs, especially during cementogenesis, might be utilized for the development of strategies aimed the endodontic regeneration and periodontal re-attachment. Procuring human DF-HERSCs can facilitate HERS-associated studies.

---

✉ Jin-Kyu Yi  
jink.yi@khu.ac.kr

<sup>1</sup> Anesthesia and Pain Research Institute, School of Medicine, Yonsei University, Seoul, South Korea

<sup>2</sup> Department of Conservative Dentistry, School of Dentistry, Kyung Hee University, Seoul, South Korea

<sup>3</sup> Department of Conservative Dentistry, Kyung Hee University Dental Hospital at Gangdong, 892, Dongnam-Ro, Gangdong-Gu, Seoul 05278, South Korea

## Introduction

The development of the tooth is based on the interactions between oral epithelium and ectomesenchyme [1]. Odontogenesis begins with the invagination of the oral epithelium, followed by subsequent events such as mesenchymal condensation at the border of the developing tooth bud [2], cell proliferation, differentiation. The inner and outer enamel epithelium, cervical loop, and Hertwig’s epithelial root sheath (HERS) belong to the odontogenic epithelium. The inner and outer enamel epithelia proliferate at the cervical loop and can fuse. HERS is formed by the fusion of the inner and outer enamel epithelia. After the secretion of pre-dentin matrix, HERSCs migrate away from the root surface, undergo apoptosis, or remain in the DF [3]. Understanding the bioactive effects of odontogenic epithelium on mesenchymal cells might unveil the underlying mechanism of tissue regeneration [4].

Regenerative endodontic procedures (REPs) induce continuous development of the root in necrotic immature teeth. The growth of immature necrotic tooth is caused by the deposition of cementum-like tissue [5, 6]. Those data suggest the relevance of cementogenesis during REPs. Cementogenesis is also a critical process for periodontal tissue regeneration. The periapical region of immature teeth is known to comprise the DF, dental papilla, and periodontal ligament (PDL), with these tissues containing the precursors of dental mesenchymal stem cells (dMSCs) [7, 8]. Dental follicle cells (DFCs) contain potent precursors of cementoblasts and HERSCs regulate the cementoblastic differentiation of the DFCs [9]. HERSCs also could undergo cementoblastic differentiation through EMT and form cementum-like tissue [10, 11]. Collectively, it can be hypothesized that cementum-forming dMSCs and HERSCs are responsible for the continuous development of the root during REPs. Interactions between HERSCs and DFCs during REPs or periodontal tissue regeneration are being highlighted [12].

Most studies on HERS have used rodent-derived HERSCs, as ethical issues restrict access to developing human teeth. Human HERSCs have been isolated from PDL [9, 13]. A small number of HERSCs are found in PDL, and their isolation has not always been successful or efficient. Procuring of human HERSCs remains a challenge in the study of HERSCs.

Dental follicle (DF) is a loose connective tissue surrounding the enamel organ and dental papilla in the developing tooth germ and is composed of precursors of cementoblasts, PDL cells (PDLs), and osteoblasts. Notably, DF disappears as the tooth erupts; however, DF can often be found in the impacted tooth [14]. DF resides between an impacted tooth and the alveolar socket. The shape and size of DF are irregular and are not present in all impacted teeth. Morsczek et al. reported the isolation of mesenchymal precursors from human DF in 2005. [15]

In this study, we hypothesized that DF contains an epithelial population that can be regarded as HERSCs. The aim of this study was the isolation and characterization of the epithelial population from DF, named DF-HERSCs. As such, DF might substitute PDL tissues with respect to isolation of HERSCs. Procuring DF-HERSCs can facilitate the study of HERS aiming endodontic and periodontal regeneration. To the best of our knowledge, this is the first study reporting the isolation of HERSCs from human DF.

## Materials and methods

### Cells and cell culture

Primary DF-HERSCs and DFCs were prepared from DF. NHEKs and normal human epidermal fibroblasts (NHEFs) were isolated from the foreskin. NHOKs and PDLs were

isolated from gingival and PDL tissues, respectively. This study was approved by the Institutional Review Board Kyung Hee University Hospital at Gang-dong (IRB Approval No. KHNMC 2017-06-009). Informed consent was obtained from the subjects or the parents of subjects under 19 years of age. For isolation of DF-HERSCs, DFs were collected from impacted third molars obtained after surgical extraction at the Department of Oral and Maxillofacial Surgery, Kyung Hee University Dental Hospital, at Gang-Dong, Seoul, Korea. Isolation of single cells from DF was performed as described previously [16]. Briefly, DF was minced and treated with 1 mg/mL collagenase type I (Gibco, Grand Island, NY, USA) and 2.4 mg/mL Dispase (Gibco) for 1 h at 37 °C. The single-cell suspension was collected after treatment with 0.05% trypsin-EDTA (Gibco) for 15 min at 37 °C and filtered using a 40- $\mu$ m strainer (Falcon, NC, USA). The enzymes were inactivated using keratinocyte serum-free medium (SFM; Gibco) with 10% FBS (Gibco), and then the single-cell suspension was plated. The medium was changed every day until the emergence of epithelial colonies. Epithelial populations were selected with keratinocyte SFM. Mesenchymal populations did not survive, and only epithelial populations survived in the presence of keratinocyte SFM.

Primary NHOKs and NHEKs were prepared according to the methods described elsewhere [17]. DF-HERSCs, NHOKs, and NHEKs were maintained in keratinocyte SFM (Gibco) with the following supplements: 2.5  $\mu$ g human recombinant epidermal growth factor (EGF; Gibco), 25 mg bovine pituitary extract (Gibco), and 1% penicillin/streptomycin (P/S; ScienCell, Carlsbad, CA, USA). DFCs and PDLs were cultured in  $\alpha$ MEM (Gibco) supplemented with 10% FBS (Gibco) and 1% P/S (ScienCell). Differentiation and mineralization of cells were induced with  $\alpha$ MEM-based osteogenic medium ( $\alpha$ MEM-M) that contains the following:  $\alpha$ MEM medium supplemented with 10% FBS, 5 mg/mL gentamicin, 100  $\mu$ M L-ascorbic acid 2-phosphate, 1.8 mM KH<sub>2</sub>PO<sub>4</sub>, and 10 mM  $\beta$ -glycerol phosphate (Sigma-Aldrich). NHEFs were maintained in Dulbecco's modified Eagle medium (WELGEN, Seoul, Korea) with 10% FBS (Gibco) and 1% P/S (ScienCell).

### Western blotting

Total protein concentration was determined using Quick Start Bradford reagent (Bio-Rad, Hercules, CA, USA). Western blot analysis was performed using the following antibodies: rabbit monoclonal anti-p16<sup>INK4A</sup> (1:2000, Cell Signaling Technology, Danvers, MA, USA); mouse monoclonal anti-N-Cadherin (1:500, Santa Cruz Biotechnology, Santa Cruz, CA, USA); mouse monoclonal anti-E-Cadherin (1:1000, Santa Cruz Biotechnology); mouse monoclonal anti-p63 (1:1000, Abcam, Cambridge, UK); mouse monoclonal anti-Involucrin (1:2000, Sigma-Aldrich, St. Louis, MO, USA);

and mouse monoclonal anti-GAPDH (1:2000, Santa Cruz Biotechnology). Chemiluminescence signals were detected using the HyGLO chemiluminescent HRP antibody detection reagent (Denville Scientific Inc., Metuchen, NJ, USA).

### Polymerase chain reaction

Total RNA was extracted using the RNeasy Mini Kit (Qiagen, Hilden, Germany). Reverse transcription of RNA was performed with 2.5 µg total RNA using the AccuPower RT PreMix (Bioneer, Daejeon, Korea). Subsequently, polymerase chain reaction (PCR) was performed with AccuPower GoldHotstart Taq PCR Premix (Bioneer) using a PCR thermocycler (Applied Biosystems, Mannheim, Germany) with the following conditions: initial denaturation at 94 °C for 2 min; 35-cycledenaturation at 94 °C for 30 s, annealing at 60 °C for 1 min, and extension at 72 °C for 1 min; and a final extension at 72 °C for 10 min. PCR products were resolved on a 1.5% agarose gel and stained with Dyne LoadingStar ethidium bromide (DYNEBIO, Seongnam, Korea). Primer sequences are detailed in Table 1.

### Quantitative reverse transcriptase polymerase chain reaction

Isolated messenger RNA (mRNA) was reverse-transcribed to cDNA using RNA to cDNA EocDry™ Premix (Oligo dT) System (Takara Bio, Kusatsu, Japan). Accordingly, cDNA was converted using oligo dT primers with the SMART® MMLV reverse transcriptase (Takara Bio). Subsequently, quantitative reverse-transcriptase PCR (qPCR) was performed

using a StepOnePlus™ system (Bio-Rad) with the SYBR™ Green Master Mix (Applied Biosystems) in the following conditions: initial denaturation at 94 °C for 30 s; 40 cycles of denaturation at 94 °C for 5 s and annealing at 58 °C for 30 s; and a final extension at 60 °C for 5 min. Primer sequences are detailed in Table 1.

### Preparation of DFC-conditioned medium

DFCs were cultured to 70–80% confluency in 100-mm culture dishes. Cells were washed twice with PBS and incubated keratinocyte SFM without supplements for 48 h. The supernatant was collected and centrifuged at 288×g for 3 min. The DFC-conditioned medium (DFC-CM) was filtered using a 0.2-µm pore filter (Nalgene, Rochester, NY, USA) and stored at either 4 °C or –20 °C for long-term storage.

### Induction of epithelial-mesenchymal transition in DFHERSCs

DF-HERSCs, NHOKs, and NHEKs were treated with 5 ng/mL of TGF-β (PeproTech, Rocky Hill, NJ, USA) for 10 days. Morphologic changes were observed under a light microscope. Cells were harvested for Western blotting and qPCR analysis at day 10.

### Alkaline Phosphatase Staining

The acquisition of osteogenic potency after the progression of EMT was evaluated with APL staining. Cells were treated according to two distinct methods: TGF-β treatment or

**Table 1** Primers used in PCR and RT-PCR

Gene	Sequence, F: Forward (5'–3'), R: Reverse (3'–5')	Size (bp)	Annealing temp (°C)
CD14	F: 5'-CCTGCTCTCTTGTAATGATATAGCC-3'	25	63.7
	R: 3'-GCCCAGTCCAGGATTGTCAG-5'	20	
CD31	F: 5'-CCACATACACTCCTTCCACCAA-3'	22	64.5
	R: 3'-TTGCCCTGGATCTCCTCTTG-5'	20	
CD29	F: 5'-CTGAAGACTATCCCATTGACCTCTA-3'	25	64.1
	R: 3'-GCTAATGTAAGGCATCACAGTCTTT-5'	25	
CD73	F: 5'-AACCACGTATCCATGTGCAT-3'	20	62.1
	R: 3'-CACTTGGTGCAAAGAATCT-5'	21	
CD90	F: 5'-ACCCAGTCCAGATCCA-3'	17	62.4
	R: 3'-GTTAGGCTGGTCACCTTCTG-5'	20	
AMBN	F: 5'-ACTGTCTCATTGTCTCAAGGC-3'	21	62.6
	R: 3'-GGACCTGATACTGATCCTATGC-5'	22	
AMELX	F: 5'-TGATAGCCTGAGAATGTGAGTTC-3'	23	62.9
	R: 3'-GATTTTATTTGCCTGCCTCTG-5'	22	
ENAM	F: 5'-GGTGGTAACCTCTGTGGAAT-3'	20	62.3
	R: 3'-GAAGCAGCCATCACATAATCAAC-5'	23	
GAPDH	F: 5'-TGATGTTGAGGTCAATGAAGGG-3'	22	62.8
	R: 3'-ACATCGCTCAGACACCATG-5'	19	

culturing with  $\alpha$ MEM. First, EMT was induced for 10 days by treatment of 5 ng/mL of TGF- $\beta$  in DF-HERSCs, NHOKs, and NHEKs under keratinocyte SFM. Keratinocyte SFM was changed at 10 days with  $\alpha$ MEM and  $\alpha$ MEM-OM and maintained for 7 days until performing the ALP staining. Second, DF-HERSCs, NHOKs, and NHEKs were maintained under various media; keratinocyte SFM,  $\alpha$ MEM, and  $\alpha$ MEM-OM for 7 days and performed ALP staining. For ALP staining, cells were washed three times with PBS-T. ALP staining was performed according to the manufacturer's protocol of StemTAGTM Alkaline Phosphatase Staining Kit (CELL BIOLABS, INC., CA, USA).

### Alizarin red staining

DF-HERSCs, NHOKs, and NHEKs were maintained under various media: keratinocyte SFM,  $\alpha$ MEM, and  $\alpha$ MEM-OM for 19 days. Cells were washed with PBS and fixed with 4% paraformaldehyde for 15 min at room temperature. 2% ARS solutions were added to the fixed cells and maintained in slow-shaking motion for 30 min at room temperature. The cells were then washed with distilled water 3 times. The staining images were visualized using a Zeiss Axiovert 200 (Carl Zeiss Microscopy, Jena, Germany).

### Statistical analysis

All data from the in vitro experiments are expressed as means (standard deviation) and were analyzed using Student's *t* test and one-way analysis of variance (ANOVA) followed by Bonferroni's multiple comparison test or repeated measures ANOVA *t* test. *p* value <0.05 was considered to indicate statistically significant differences.

## Results

### Dental follicle contains epithelial populations

Dental follicle, gingival tissue, and foreskin were harvested from patients for isolation of single cells (Fig. 1a). DF-HERSCs appeared at 7–10 days after plating of single-cell suspensions (Fig. 1b). DF-HERSCs, NHOKs, and NHEKs were observed as homogenous monolayers of polygonal cells with a cobblestone-shaped appearance (Fig. 1c). DFCs had a spindle-shaped fibroblast-like morphology, indicating a mesenchymal phenotype. The epithelial phenotype of DF-HERSCs was further verified at the molecular level by Western blotting of epithelial-mesenchymal markers. Specifically, E-cadherin and

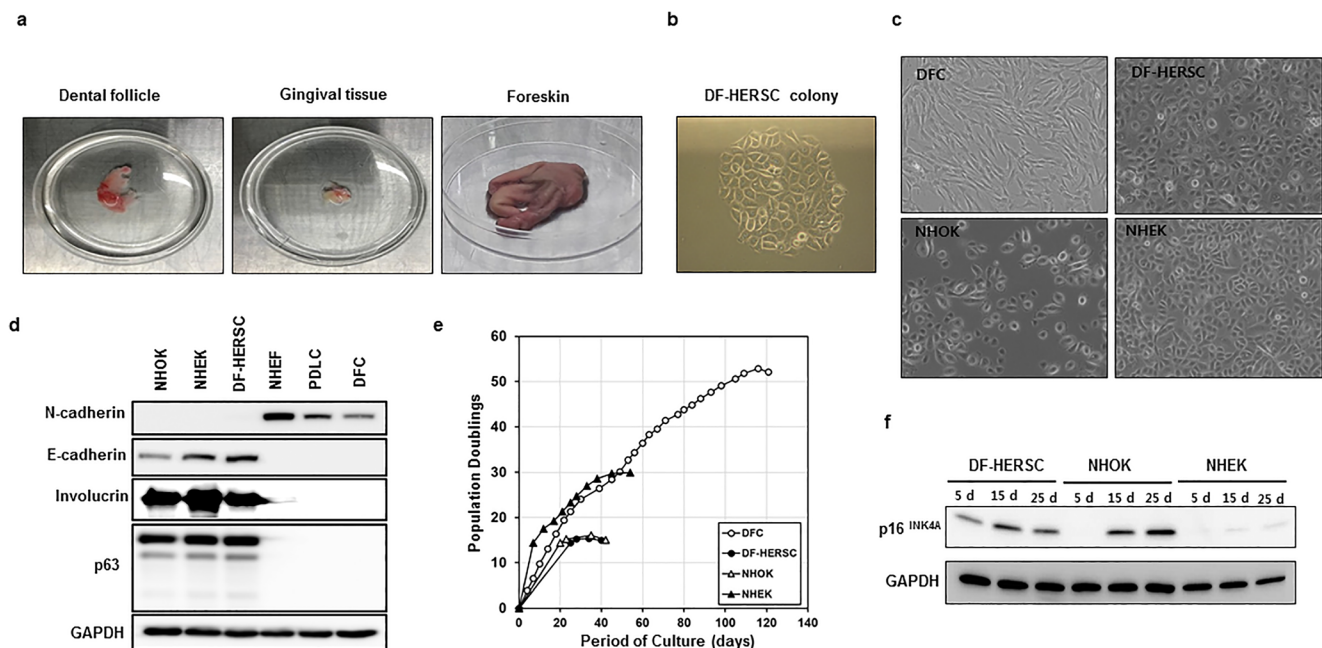


**Fig. 1** The DF contains populations of epithelial cells. **a** DF, gingival tissue, and foreskins were harvested for isolation of primary cells. **b** Epithelial-like colonies appeared at 7–10 days after plating the DF-derived single-cell suspensions. **c** DF-HERSCs, NHOKs, and NHEKs demonstrated polygonal and cobblestone-shaped morphologies. DFCs showed a spindle-shaped appearance. **d** Western blot analysis was performed against epithelial and mesenchymal markers. Both E-cadherin

and p63 were expressed, whereas N-cadherin was not in DF-HERSCs, NHOKs, and NHEKs. **e** NHEKs showed a prolonged capacity for cell proliferation compared with that of DF-HERSCs and NHOKs. DFCs had the longest life span compared with other epithelial groups. **f** The expression of p16 emerged at day 5 in DF-HERSCs and at day 15 in NHOKs

p63 were shown to be expressed, whereas N-cadherin was not expressed in DF-HERSCs (Fig. 1d).

### Characteristics of DF-HERS cells

The number of colonies of DF-HERSC and NHOK was much lower than that of NHEKs. Concomitantly, the population doubling curves revealed a restricted proliferation capacity in DF-HERSCs and NHOKs compared with that in NHEKs (Fig. 1e). Of note, DFCs showed the highest ex vivo expansion capacity. The expression of p16, a senescence marker, appeared at 5 days in DF-HERSCs and at 15 days in NHOKs (Fig. 1f). In contrast, NHEKs did not exhibit any expression of p16.

PCR data showed the cellular profiles of DF-HERSCs (Fig. 2a). DF-HERSCs were shown to be negative for CD31, an endothelial marker. Human umbilical vein endothelial cells (HUVECs) which are positive for CD31 were used as a control group. DF-HERSCs also exhibit negative expression of hematopoietic markers such as CD14 and CD34. In contrast, human leukemic monocytes (THP-1) strongly expressed CD14. The expression of mesenchymal markers was confirmed based on the detection of CD29, CD73, and CD90.

DF-HERSCs, NHOKs, and NHEKs showed weak expression of CD29 and CD73 and were negative for CD90, whereas DFCs showed high expression of CD29, CD73, and CD90.

DF-HERSCs were treated with DFC-derived conditioned medium (DFC-CM) for 48 h to evaluate the effect of DFCs on the expression of enamel matrix derivative (EMD)-associated genes, including ameloblastin (*AMBN*), amelogenin (*AMELX*), and enamelin (*ENAM*). EMD-associated genes were not expressed in all groups regardless of treatment with DFC-CM (Fig. 2b). Likewise, qPCR data also showed insignificant mRNA expression of EMD-associated genes (Fig. 2c).

### TGF-β triggers the progression of EMT and acquisition of osteogenic potency in DF-HERSCs

Morphological changes appeared at 10 days after treatment with TGF-β (Fig. 3a). In the TGF-β-treated group, polygonal cells were shown to attain a rounded shape. Moreover, the cytoplasm and nuclei were enlarged in both the control and TGF-β-treated groups. Some cells showed morphologic conversions resembling a fibroblast-like appearance. However, the observed morphological change was incomplete. The

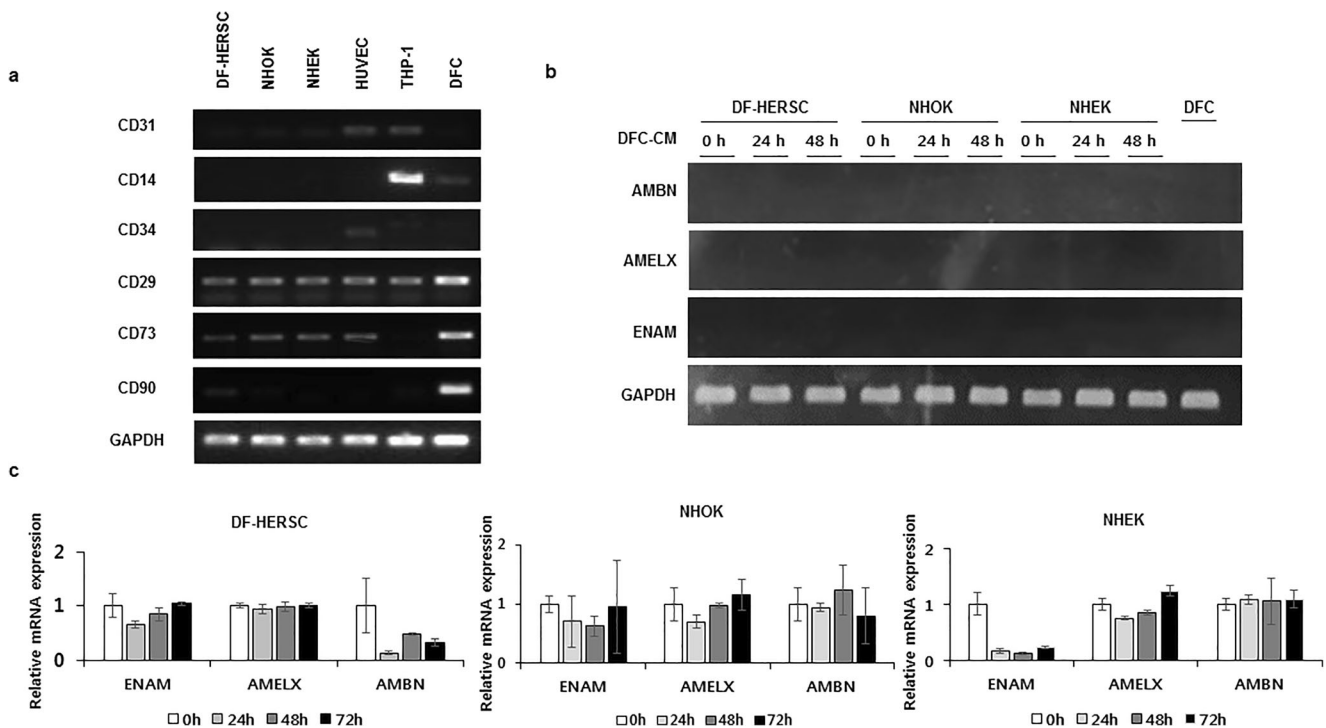


**Fig. 2** Characterization of DF-HERSCs. **a** DF-HERSCs were negative for CD31, an endothelial marker. HUVECs and THP-1 showed weak expression of CD31. DF-HERSCs were also negative for CD14 and CD34, which are hematopoietic markers. In contrast, THP-1 cells showed a significant expression of CD14. NHOKs and NHEKs were also negative for CD31, CD14, and CD34, as observed with DF-HERSCs. Mesenchymal markers analyzed included CD29, CD73, and CD90. DF-HERS, NHOKs, and NHEKs were weakly positive for CD29 and

CD73 compared with DFCs. DF-HERSCs, NHOKs, and NHEKs were negative for CD90. DFCs were positive to CD29, CD73, and CD90. **b** Treatment with DFC-CM did not alter the expression of EMD-associated genes, including ameloblastin (*AMBN*), amelogenin (*AMELX*), and enamelin (*ENAM*) in DF-HERSCs, NHOKs, and NHEKs. **c** Results of qPCR analysis demonstrated that treatment with DFC-CM did not promote the mRNA expression of *AMBN*, *AMELX*, and *ENAM* in DF-HERSCs, NHOKs, and NHEKs

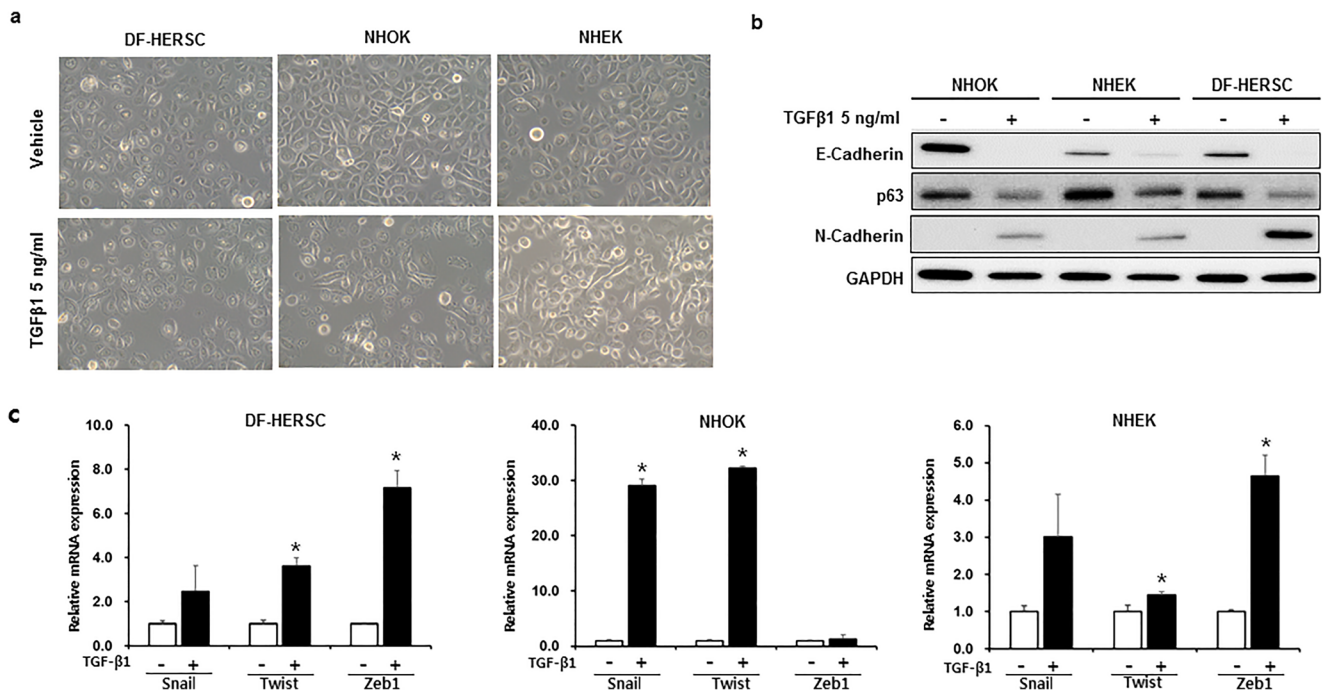


**Fig. 3** Treatment with TGF- $\beta$  promotes the progression of EMT in DF-HERSCs. **a** Polygonal cells became round and some cells showed bipolar process-like appearance resembling the morphology of the mesenchymal cells. However, the morphological transition was incomplete. **b** Expression of E-cadherin disappeared, whereas N-cadherin was

expressed after treatment with TGF- $\beta$  in DF-HERSCs, NHOKs, and NHEKs. The expression of N-cadherin was more pronounced in DF-HERSCs than in NHOKs and NHEKs. **c** The relative mRNA expression of EMT-associated transcription factors, including Snail, Twist, and ZEB1 increased upon treatment with TGF- $\beta$

progression of EMT was also evaluated at the molecular level by Western blot analysis (Fig. 3b). Treatment with TGF- $\beta$  was found to induce loss of the expression of E-cadherin, an epithelial marker, resulting in activation of the N-cadherin expression in DF-HERS, NHOK, and NHEK cells. Furthermore, the expression of p63, a hallmark of the epithelial phenotype, was shown to be decreased in the TGF- $\beta$ 1-treated group. Quantitative PCR analysis also demonstrated that treatment with TGF- $\beta$  could result in increased expression of EMT-regulating transcription factors (Fig. 3c). The mRNA expression of Runx2 was enhanced by TGF- $\beta$  treatment for 10 days (Fig. 4a). DF-HERSCs, NHOKs, and NHEKs that were cultured with  $\alpha$ MEM or  $\alpha$ MEM-osteogenic medium ( $\alpha$ MEM-OM) after progression of EMT were positive to ALP staining (Fig. 4b).

### **$\alpha$ MEM supplemented with FBS triggers the progression of EMT and acquisition of osteogenic potency in DF-HERSCs**

DF-HERSCs that were maintained under  $\alpha$ MEM showed significant morphologic changes (Fig. 4c). DF-HERSCs lost cobblestone shape and became elongated, resembling the shape of a mesenchymal cell. DF-HERSCs that were maintained under  $\alpha$ MEM and  $\alpha$ MEM-OM demonstrated the progression of EMT and osteogenic differentiation. The expression of EMT-regulating genes, including Snail, Twist, and

Zeb1, increased in  $\alpha$ MEM and  $\alpha$ MEM-OM groups (Fig. 4d). The expression of osteogenic markers, such as Runx2, ALP, DSPP, and CEMP-1, also increased in  $\alpha$ MEM and  $\alpha$ MEM-OM groups (Fig. 5a). HERSCs, NHOKs, and NHEKs were positive to ALP staining in  $\alpha$ MEM and  $\alpha$ MEM-OM groups (Fig. 5b). Differentiation and calcification of DF-HERSs, NHOKs, and NHEKs were confirmed by Alizarin red staining. Calcified nodules were deposited in  $\alpha$ MEM and  $\alpha$ MEM-OM group (Fig. 5c).

## **Discussion**

Odontogenic epithelium originates from invaginated oral epithelium. Its name differs depending on the developmental stages, for example, the inner and outer enamel epithelium, cervical loop, HERS, and epithelial rests of Malassez. Previous studies have highlighted the regulatory roles of odontogenic epithelium on the function of ectomesenchyme during crown and root formation [18, 19]. Regarding the development of the root, HERS and dMSCs are responsible for the formation of the cementum and PDL [20–22]. HERS has been shown to regulate the formation of cementum either directly or indirectly [20, 23]. Similarly, studies have revealed the possible involvement of HERS during REPs of the immature necrotic tooth [24], with the survival of HERS being regarded as a critical factor for favorable clinical outcomes.

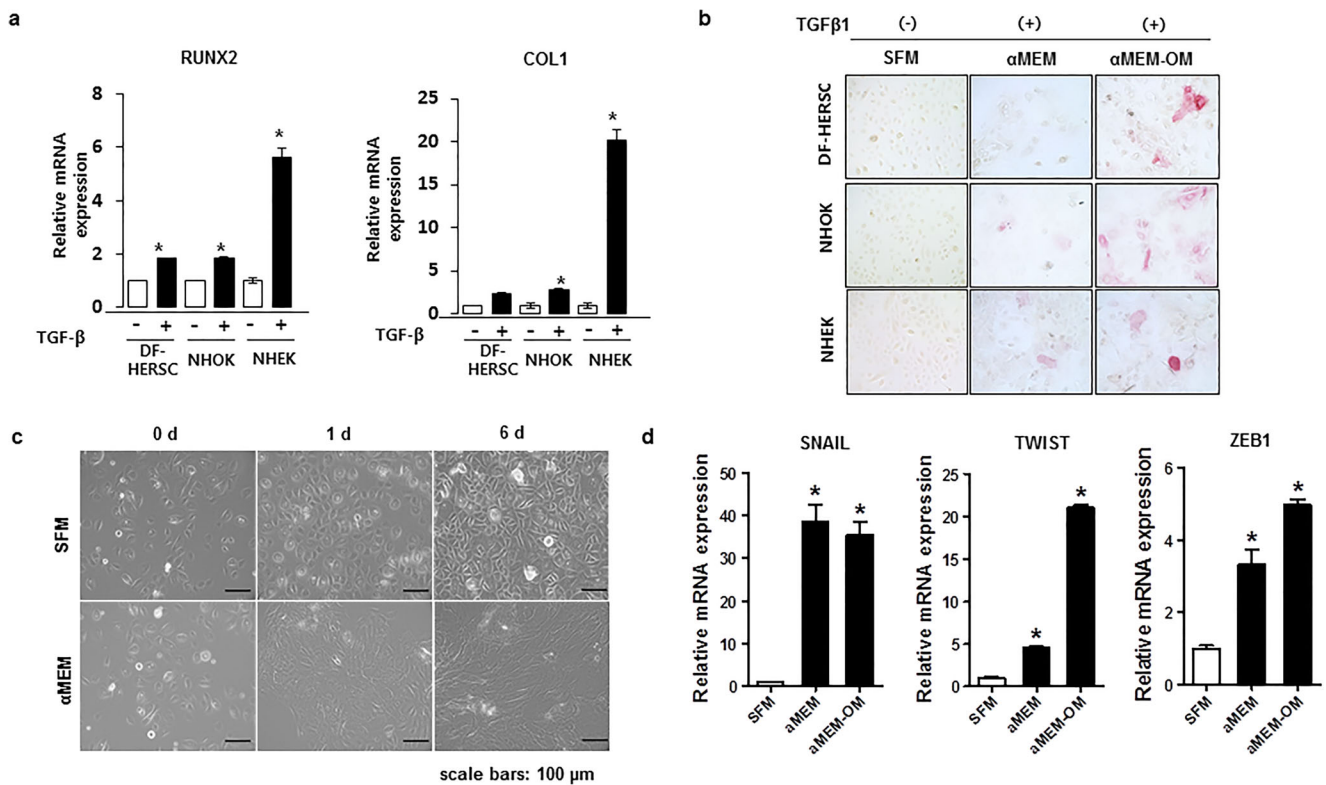


**Fig. 4** Acquisition of osteogenic potency after treatment with TGF-β and progression of αMEM-induced EMT. **a** The relative mRNA Expression of Runx2 increased after treatment with TGF-β in DF-HERSCs, NHOKs, and NHEKs. **b** DF-HERSCs, NHOKs, and NHEKs that were treated with TGF-β were positive to ALP staining in αMEM-OM groups. **c** DF-

HERSCs showed morphologic changes resembling EMT under αMEM conditions. DF-HERSCs lost polygonal shape and gained process-having appearance. **d** The mRNA expression of EMT-associated transcription factors such as Snail, Twist, and Zeb1 increased in DF-HERSCs under αMEM and αMEM-OM conditions

The periradicular tissue is reportedly influenced by pathologic environment, with the period of exposure to inflammatory conditions affecting the existence of vital tissue, including HERS [25]. Investigating the interactions between HERSCs and dMSCs might unveil the underlying mechanisms of endodontic regeneration. Accordingly, HERS-derived bioactive molecules could be utilized for controlling of REP, aiming at predictable clinical outcomes regardless of the survival of HERS.

Procuring human-derived HERSCs is a prerequisite for the study of HERSC-dMSC interactions. Harvesting HERSCs from PDL was inefficient for gaining enough cell stocks. The DF is a connective tissue surrounding the developing tooth, with its subpopulations expressing cellular markers of the embryonic stem, mesenchymal stem, neural crest stem, and glial cells [14]. Initially, we hypothesized that DF might also contain populations of epithelial cells that could be defined as HERSCs. However, to date, definite markers for HERSCs are not available. Nevertheless, DF-derived epithelial cells could be regarded as DF-HERSCs based on the following backgrounds. First, populations of epithelial cells in the periodontium were shown to originate from the oral epithelium. Second, epithelial compartments during odontogenesis are named according to the developmental

stage of the tooth. Third, we harvested DF from teeth with an almost fully grown root. Fourth, EMD-associated genes were not expressed in DF-derived epithelial cells.

Epithelial cells were isolated from human DF (Fig. 1a, b), named DF-HERSCs. The epithelial phenotype of DF-HERSCs was confirmed by both morphological and Western blot analyses (Fig. 1c, d). DF-HERS cells were shown to be neither endothelial nor hematopoietic (Fig. 2a), coinciding with the results of other studies on HERS [13, 16, 26]. DF-HERSCs were also shown to express low levels of mesenchymal markers such as CD29 and CD73. Similarly, other studies have demonstrated that human HERSCs express low levels of mesenchymal markers such as CD29, CD44, CD73, CD90, and CD105 [13, 16, 26]. Compared with NHEKs, oral epithelial cells were reported to have limited proliferative capacity (Fig. 1e). Moreover, DF-HERSCs and NHOKs showed early emergence of p16 compared with NHEKs (Fig. 1f), in agreement with other studies that report the limited ex vivo life span of HERSCs [27]. According to the population doubling curve, the period of culture of DF-HERSCs (Fig. 1e) was similar to that of PDL-HERSCs described by Nam et al. in 2011 [16]. The expression of EMD-associated genes was absent in DF-HERSCs and was shown to be unaffected by DFC-CM (Fig. 2b, c). Accordingly, the

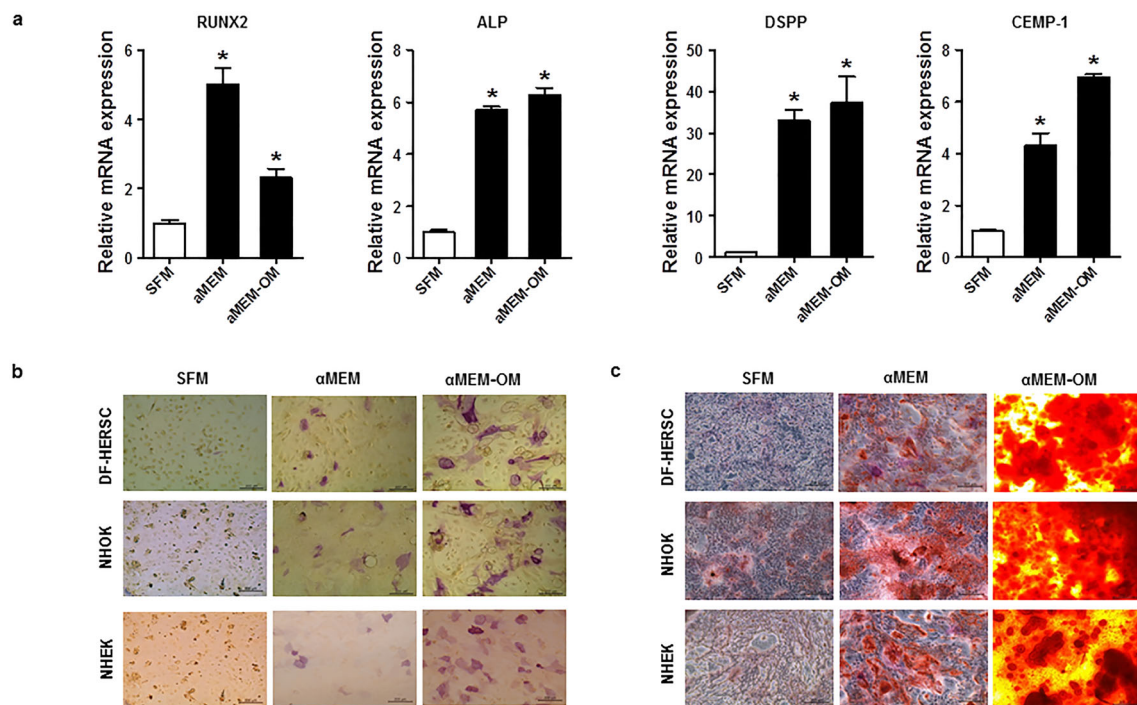


**Fig. 5** αMEM and αMEM-OM trigger the progression of EMT and the acquisition of osteogenic potency in DF-HERSCs, NHOKs, and NHEKs. **a** The mRNA expressions of osteogenic markers, such as Runx2, ALP, DSPP, and CEMP-1, were increased in DF-HERSCs that were cultured in αMEM and αMEM-OM. **b** DF-HERSCs, NHOKs, and NHEKs were

positive to ALP staining in αMEM, and αMEM-OM groups. Response to ALP staining was prominent in αMEM-OM groups. **c** Formation of mineralized nodules was observed in αMEM, and αMEM-OM groups. αMEM-OM groups were significantly positive to Alizarin red staining

lack of amelogenin expression was reported in a previous HERS study [13]. Considering the developmental stage of the tooth, the emergence of the cervical loop implies the completion of the crown portion, whereas the presence of HERS indicates the initiation of root development. The expression of enamel-associated genes was high in cervical-loop cells compared with that in HERSCs [28]. Ameloblasts have been reported to undergo DFC-induced apoptosis [29], with HERSCs being capable of forming enamel at the initial developmental stage. As the development of tooth progresses, enamel-associated genes are switched off whereas root-forming signals are switched on in HERSCs. Cervical-loop cells are known to generate enamel-like tissues, whereas HERSCs form the cementum and structure of PDL. Collectively, these data demonstrate the time-dependent functional transition of the odontogenic epithelium and the switch-on/switch-off effects with respect to regulating genes during odontogenesis. Loss of expression of EMD-associated genes implies the developmental stages of DF-derived epithelial cells and deserv-ing the DF-derived epithelial cells as DF-HERSCs.

Human and rat studies have revealed that HERSCs undergo EMT upon treatment with TGF-β [30, 31]. EMT progression is a critical process for the tissue-forming function in HERSCs. These cells are known as cementoblastic precursors and form cementum-like tissues through EMT during in vivo transplantations [23]. In this study, DF-HERSCs

showed the capacity for progression of EMT, but the observed morphological changes in DF-HERSCs, NHOKs, and NHEKs after treatment with TGF-β1 were not significant (Fig. 3a). Treatment with TGF-β partly decreased the expression of p63 (Fig. 3b), implying the existence of various EMT pathways. In this study, maintenance of DF-HERSCs with αMEM supplemented with FBS also induced the progression of EMT. (Fig. 4c, d) DF-HERSCs, NHOKs, and NHEKs undergo osteogenic differentiation and calcification when they were cultured with an αMEM-based osteogenic induction medium. (Fig. 5b, c) In HERS studies, rodent-derived HERSCs are cultured in epithelial cell medium supplemented with FBS. Interestingly, human epithelial cells, including HERSCs, NHOKs, and NHEKs, are cultured in a serum-free medium. DF-HERSCs, NHOKs, and NHEKs cannot survive in αMEM-based media without FBS. Due to this, no αMEM without the FBS group was included in this study.

The acquisition of stem-like properties after progression of EMT is a characteristic of epithelial cells [32]. Differentiation of DF-HERSCs into cementoblasts could be explained by the newly acquired stemness through the EMT. In this study, αMEM-induced calcifying potency of DF-HERSCs seems to be potent and efficient. Therefore, to directly control the direct conversion of DF-HERSCs to hard tissue-forming cells could be a strategy for cementum regeneration.



DF-HERSCs were compared with NHOKs, a control oral epithelium, and NHEKs, a non-oral epithelium, to assess whether HERSC-associated features are oral epithelium-specific or common epithelial characteristics. DF-HERSCs showed common features with NHOKs and NHEKs including, EMT progression, acquisition of osteogenic differentiation capacity, and expression profiles of mesenchymal markers and enamel matrix derivative (EMD)-associated genes. Further study is required to investigate the functional specificity of DF-HERSCs in the interactions with dMSCs.

## Conclusions

DF contains putative populations of HERSC, named DF-HERSC. DF-HERSCs shared common characteristics with NHOKs and NHEKs, including EMT progression, acquisition of osteogenic differentiation capacity after progression of EMT, and expression profiles of mesenchymal markers and enamel matrix derivative (EMD)-associated genes.

**Acknowledgments** Professor Dong-Mok Ryu kindly provided tissues for primary culture.

**Funding Information** This study was supported by the grants from the National Research Foundation of Korea (NRF) funded by the Korean government (NRF-2017R1C1B2008406) and Kyung Hee University in 2017(KHU-20170853).

## Compliance with Ethical Standards

**Conflict of Interest** The authors declare that they have no conflict of interest.

**Ethical approval** All procedures performed in studies involving human participants were in accordance with the ethical standards of the institutional and/or national research committee and with the 1964 Helsinki declaration and its later amendments or comparable ethical standards.

**Informed consent** Informed consent was obtained from all individual participants included in the study.

## References

- Guo Y, Guo W, Chen J, Chen G, Tian W, Bai D (2018) Are Hertwig's epithelial root sheath cells necessary for periodontal formation by dental follicle cells? *Arch Oral Biol* 94:1–9. <https://doi.org/10.1016/j.archoralbio.2018.06.014>
- Tucker A, Sharpe P (2004) The cutting-edge of mammalian development; how the embryo makes teeth. *Nat Rev Genet* 5:499–508. <https://doi.org/10.1038/nrg1380>
- Hand AR, Frank ME (2015) *Fundamentals of oral histology and physiology*. John Wiley & Sons
- Choung HW, Lee DS, Park YH, Lee YS, Bai S, Yoo SH, Lee JH, You HK, Park JC (2019) The effect of CPNE7 on periodontal regeneration. *Connect Tissue Res* 60:419–430. <https://doi.org/10.1080/03008207.2019.1574776>
- Shimizu E, Ricucci D, Albert J, Alobaid AS, Gibbs JL, Huang GT, Lin LM (2013) Clinical, radiographic, and histological observation of a human immature permanent tooth with chronic apical abscess after revitalization treatment. *J Endod* 39:1078–1083. <https://doi.org/10.1016/j.joen.2013.04.032>
- Becerra P, Ricucci D, Loghin S, Gibbs JL, Lin LM (2014) Histologic study of a human immature permanent premolar with chronic apical abscess after revascularization/revitalization. *J Endod* 40:133–139. <https://doi.org/10.1016/j.joen.2013.07.017>
- Komaki M, Iwasaki K, Arzate H, Narayanan AS, Izumi Y, Morita I (2012) Cementum protein 1 (CEMP1) induces a cementoblastic phenotype and reduces osteoblastic differentiation in periodontal ligament cells. *J Cell Physiol* 227:649–657. <https://doi.org/10.1002/jcp.22770>
- Nemoto E, Sakisaka Y, Tsuchiya M, Tamura M, Nakamura T, Kanaya S, Shimonishi M, Shimauchi H (2016) Wnt3a signaling induces murine dental follicle cells to differentiate into cementoblastic/osteoblastic cells via an osterix-dependent pathway. *J Periodontol Res* 51:164–174. <https://doi.org/10.1111/jre.12294>
- Jung HS, Lee DS, Lee JH, Park SJ, Lee G, Seo BM, Ko JS, Park JC (2011) Directing the differentiation of human dental follicle cells into cementoblasts and/or osteoblasts by a combination of HERS and pulp cells. *J Mol Histol* 42:227–235. <https://doi.org/10.1007/s10735-011-9327-5>
- Sonoyama W, Seo BM, Yamaza T, Shi S (2007) Human Hertwig's epithelial root sheath cells play crucial roles in cementum formation. *J Dent Res* 86:594–599. <https://doi.org/10.1177/154405910708600703>
- Itaya S, Oka K, Ogata K, Tamura S, Kira-Tatsuoka M, Fujiwara N, Otsu K, Tsuruga E, Ozaki M, Harada H (2017) Hertwig's epithelial root sheath cells contribute to formation of periodontal ligament through epithelial-mesenchymal transition by TGF-beta. *Biomed Res (Tokyo, Japan)* 38:61–69. <https://doi.org/10.2220/biomedres.38.61>
- Huang X, Bringas P Jr, Slavkin HC, Chai Y (2009) Fate of HERS during tooth root development. *Dev Biol* 334:22–30. <https://doi.org/10.1016/j.ydbio.2009.06.034>
- Farea M, Halim AS, Abdullah NA, Lim CK, Mokhtar KI, Berahim Z, Mokhtar K, Rani AQ, Husein A (2013) Isolation and enhancement of a homogenous in vitro human Hertwig's epithelial root sheath cell population. *Int J Mol Sci* 14:11157–11170. <https://doi.org/10.3390/ijms140611157>
- Li B, Chen X, Jin Y (2018) *Tooth and dental pulp regeneration*. In: Chen X-D (ed) Book title. Elsevier
- Morszczek C, Gotz W, Schierholz J, Zeilhofer F, Kuhn U, Mohl C, Sippel C, Hoffmann KH (2005) Isolation of precursor cells (PCs) from human dental follicle of wisdom teeth. *Matrix Biol* 24:155–165. <https://doi.org/10.1016/j.matbio.2004.12.004>
- Nam H, Kim J, Park J, Park JC, Kim JW, Seo BM, Lee JC, Lee G (2011) Expression profile of the stem cell markers in human Hertwig's epithelial root sheath/epithelial rests of Malassez cells. *Mol Cells* 31:355–360. <https://doi.org/10.1007/s10059-011-0045-3>
- Calenic B, Ishkitiev N, Yaegaki K, Imai T, Costache M, Tovu M, Tovu S, Parlatescu I (2010) Characterization of oral keratinocyte stem cells and prospects of its differentiation to oral epithelial equivalents. *Romanian journal of morphology and embryology = Revue roumaine de morphologie et embryologie* 51:641–645
- Wang YH, Upholt WB, Sharpe PT, Kollar EJ, Mina M (1998) Odontogenic epithelium induces similar molecular responses in chick and mouse mandibular mesenchyme. *Dev Dyn* 213:386–397. [https://doi.org/10.1002/\(sici\)1097-0177\(199812\)213:4<386::Aid-aja4>3.0.Co;2-2](https://doi.org/10.1002/(sici)1097-0177(199812)213:4<386::Aid-aja4>3.0.Co;2-2)
- Thesleff I (2003) Epithelial-mesenchymal signalling regulating tooth morphogenesis. *J Cell Sci* 116:1647–1648. <https://doi.org/10.1242/jcs.00410>

20. Yang Y, Ge Y, Chen G, Yan Z, Yu M, Feng L, Jiang Z, Guo W, Tian W (2014) Hertwig's epithelial root sheath cells regulate osteogenic differentiation of dental follicle cells through the Wnt pathway. *Bone* 63:158–165. <https://doi.org/10.1016/j.bone.2014.03.006>
21. Bai Y, Bai Y, Matsuzaka K, Hashimoto S, Fukuyama T, Wu L, Miwa T, Liu X, Wang X, Inoue T (2011) Cementum- and periodontal ligament-like tissue formation by dental follicle cell sheets cocultured with Hertwig's epithelial root sheath cells. *Bone* 48:1417–1426. <https://doi.org/10.1016/j.bone.2011.02.016>
22. Bosshardt DD, Stadlinger B, Terheyden H (2015) Cell-to-cell communication—periodontal regeneration. *Clin Oral Implants Res* 26:229–239. <https://doi.org/10.1111/clr.12543>
23. Xiong J, Mrozek K, Gronthos S, Bartold PM (2012) Epithelial cell rests of Malassez contain unique stem cell populations capable of undergoing epithelial-mesenchymal transition. *Stem Cells Dev* 21:2012–2025. <https://doi.org/10.1089/scd.2011.0471>
24. Songtrakul K, Azarpajouh T, Malek M, Sigurdsson A, Kahler B, Lin LM (2020) Modified apexification procedure for immature permanent teeth with a necrotic pulp/apical periodontitis: a case series. *J Endod* 46:116–123. <https://doi.org/10.1016/j.joen.2019.10.009>
25. Chrepa V, Pitcher B, Henry MA, Diogenes A (2017) Survival of the apical papilla and its resident stem cells in a case of advanced pulpal necrosis and apical periodontitis. *J Endod* 43:561–567. <https://doi.org/10.1016/j.joen.2016.09.024>
26. Nam H, Kim JH, Kim JW, Seo BM, Park JC, Kim JW, Lee G (2014) Establishment of Hertwig's epithelial root sheath/epithelial rests of Malassez cell line from human periodontium. *Mol Cells* 37:562–567. <https://doi.org/10.14348/molcells.2014.0161>
27. Shinmura Y, Tsuchiya S, Hata K, Honda MJ (2008) Quiescent epithelial cell rests of Malassez can differentiate into ameloblast-like cells. *J Cell Physiol* 217:728–738. <https://doi.org/10.1002/jcp.21546>
28. Guo Y, Guo W, Chen J, Tian Y, Chen G, Tian W, Bai D (2018) Comparative study on differentiation of cervical-loop cells and Hertwig's epithelial root sheath cells under the induction of dental follicle cells in rat. *Sci Rep* 8:6546. <https://doi.org/10.1038/s41598-018-24973-0>
29. Lee JH, Lee DS, Nam H, Lee G, Seo BM, Cho YS, Bae HS, Park JC (2012) Dental follicle cells and cementoblasts induce apoptosis of ameloblast-lineage and Hertwig's epithelial root sheath/epithelial rests of Malassez cells through the Fas-Fas ligand pathway. *Eur J Oral Sci* 120:29–37. <https://doi.org/10.1111/j.1600-0722.2011.00895.x>
30. Lee JH, Nam H, Um S, Lee J, Lee G, Seo BM (2014) Upregulation of GM-CSF by TGF-beta1 in epithelial mesenchymal transition of human HERS/ERM cells. *In Vitro Cell Dev Biol Anim* 50:399–405. <https://doi.org/10.1007/s11626-013-9712-3>
31. Chen J, Chen G, Yan Z, Guo Y, Yu M, Feng L, Jiang Z, Guo W, Tian W (2014) TGF-beta1 and FGF2 stimulate the epithelial-mesenchymal transition of HERS cells through a MEK-dependent mechanism. *J Cell Physiol* 229:1647–1659. <https://doi.org/10.1002/jcp.24610>
32. Oh JE, Kim RH, Shin KH, Park NH, Kang MK (2011) DeltaNp63alpha protein triggers epithelial-mesenchymal transition and confers stem cell properties in normal human keratinocytes. *J Biol Chem* 286:38757–38767. <https://doi.org/10.1074/jbc.M111.244939>

**Publisher's note** Springer Nature remains neutral with regard to jurisdictional claims in published maps and institutional affiliations.